

Influence of Laser Incident Energy on Chemical Composition, Crystal Structure, Morphology and Band Gap of $\text{Cu}_2\text{ZnSnS}_4$ Thin Films by Pulsed Laser Deposition

Yanan Wen^{1, a}, Lin Li^{1, b}, Yan Dong^{1, c}, Min Yao^{2, d}, Qi Liang^{1, e*}

¹School of Electronic Science and Applied Physics, Hefei University of Technology, Hefei 230009, China

²School of Chemical Engineering, Hefei University of Technology, Hefei 230009, China

^ajnwyn56@126.com, ^bjiaozhoulin@163.com, ^cyandong199@yahoo.com.cn, ^dyaomin100@163.com, ^eliangqi@126.com.

Keywords: $\text{Cu}_2\text{ZnSnS}_4$; thin film; pulsed laser deposition; laser incident energy

Abstract. The $\text{Cu}_2\text{ZnSnS}_4$ (CZTS) thin films were successfully prepared on glass substrate by pulsed laser deposition (PLD) using CZTS target. The laser incident energy was varied from 3 $\text{J}\cdot\text{cm}^{-2}$ to 6 $\text{J}\cdot\text{cm}^{-2}$ at the interval of 1 $\text{J}\cdot\text{cm}^{-2}$, and its influence on chemical composition, crystal structure, morphology and band gap of CZTS thin films was investigated by energy dispersive X-ray spectroscopy (EDS), X-ray diffraction (XRD), atomic force microscopy (AFM) and ultraviolet-visible-near infrared (UV-Vis-NIR) absorption spectra, respectively. The result of EDS indicated that these CZTS thin films were Cu-rich and S-poor. The XRD study showed CZTS thin films exhibited strong preferential orientation of grains along [112] direction. The band gap of CZTS thin films was 1.72, 1.37, 1.25 and 1.11 eV corresponding to incident laser energy of 3, 4, 5 and 6 $\text{J}\cdot\text{cm}^{-2}$.

Introduction

$\text{Cu}_2\text{ZnSnS}_4$ (CZTS) was one of the most interesting material for absorber layer of low-price thin film solar cells because of its suitable optical band gap of about 1.5 eV and its large absorption coefficient of over 10^4 cm^{-1} [1, 2]. The preparation of CZTS thin films was widely investigated, such as atom beam sputtering [3], sulfurization of electron-beam-evaporated precursors [4], co-evaporation [5], spray pyrolysis [6], RF (radio frequency) magnetron sputtering [7], hybrid sputtering [8], electrodeposition [9], thermal evaporation [10], and pulsed laser deposition (PLD) [11-13]. The solid-state reaction of the mixing powder of Cu_2S , ZnS , and SnS_2 with 1:1:1 mol ratio was used to prepare the target in PLD, and the target directly using the CZTS nanocrystal was not reported.

In this paper, the CZTS thin films were prepared on glass substrate at the substrate temperature of 400°C using the target from the CZTS nanocrystal. The influence of laser incident energy on chemical composition, crystal structure, surface morphology and band gap of CZTS thin film was systemically investigated by energy dispersive X-ray spectroscopy (EDS), X-ray diffraction (XRD), atomic force microscopy (AFM) and ultraviolet-visible-near infrared (UV-Vis-NIR) absorption spectra, respectively.

Experimental

The CZTS nanocrystal was prepared using the hydrothermal method by the mixture of newly synthesized CuS , ZnS , and SnS precursor [14]. The target was shaped and pressed into a pellet using the CZTS nanocrystal.

CZTS thin films were deposited on glass substrates by PLD with a KrF excimer laser (Lambda Physik, COMPEXPro 102, $\lambda=248 \text{ nm}$, 20 ns pulse width). The glass substrate was ultrasonically cleaned in acetone, ethanol, deionized water for 8 min, consecutively. Then the substrate was placed parallel at distance of 50 mm from the target, which was fixed on a rotating holder with rotation at

10 rpm, during laser ablation. The glass substrates were heated to 400 °C and fixed on a rotating holder with rotation at 5 rpm. The deposition chamber was evacuated to 2.0×10^{-4} Pa using a turbo molecular pump. The laser incident energy varied from $3 \text{ J}\cdot\text{cm}^{-2}$ to $6 \text{ J}\cdot\text{cm}^{-2}$ at the interval of $1 \text{ J}\cdot\text{cm}^{-2}$, and a repetition rate was 2 Hz. The deposition time was 150 min.

The chemical composition and crystal structure of CZTS thin films were measured by EDS using Japan EDX spectrometer (JSM6490/LV, Japan) and XRD, respectively. XRD patterns were measured using $\text{CuK}\alpha$ radiation, $\lambda=0.154056 \text{ nm}$, 40 kV and 50 mA (Philips X' Pert PRO SUPER, Netherlands). A scanning rate of $0.017 \text{ }^\circ\text{s}^{-1}$ was applied to record the patterns in the 2θ range of $20\text{--}80^\circ$. The surface morphology of the CZTS thin films was observed by atomic force microscopy (AFM, CSPM 4000, China). The ultraviolet-visible-near infrared (UV-Vis-NIR) absorption spectra were measured with a double beam UV-Vis-NIR (DUV-3700, Shimadzu, Japan) in the wavelength range of 400-1400 nm at the resolution of 1 nm.

Results and discussion

Chemical composition of CZTS thin films. Figure 1 showed the chemical composition of CZTS thin films deposited at the different laser incident energy from 3 to $6 \text{ J}\cdot\text{cm}^{-2}$. Compared with that of the four laser incident energy, the chemical composition of the resulting CZTS thin film at $5 \text{ J}\cdot\text{cm}^{-2}$ was $\text{Cu}_{2.15}\text{Zn}_{1.00}\text{Sn}_{1.17}\text{S}_{3.84}$ in a nearly stoichiometric relation except slightly Cu-rich and S-poor (mole ratio of Cu to (Zn+Sn) was 0.99, mole ratio of Sn to Zn was 1.17, mole ratio of S to metal was 0.89). Also, other CZTS thin films were Cu-rich and S-poor. This was due to the difference of the four element velocities during the pulsed laser deposition. The velocities of elements depended on their mass. Cu as a lighter-mass element had a higher flow speed [13], and S element as a lighter-mass element was a volatile element, which led to the enrichment of Cu and loss of S in CZTS thin films.

Crystal structure of CZTS thin films. Figure 2 showed X-ray diffraction patterns of CZTS thin films at the different laser incident energy. The XRD pattern indicated that there was single strong peak located at $2\theta = 28.6^\circ$, corresponding to the spacings of (112) planes of CZTS, which was well consistent with the standard JCPDS data file (JCPDS NO. 26-0575). And the intensity of diffraction peaks increased with the increasing of laser incident energy.

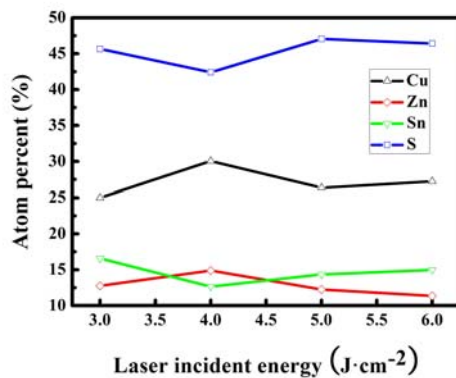


Fig.1. Chemical composition of CZTS thin films

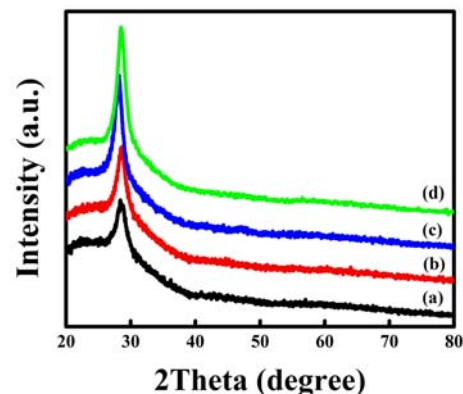


Fig.2. XRD patterns of CZTS thin films (a) $3 \text{ J}\cdot\text{cm}^{-2}$; (b) $4 \text{ J}\cdot\text{cm}^{-2}$; (c) $5 \text{ J}\cdot\text{cm}^{-2}$; (d) $6 \text{ J}\cdot\text{cm}^{-2}$

Surface morphology of CZTS thin films. Figure 3 showed AFM morphology images of CZTS thin films at the different laser incident energy. It was observed that some particles existed on the surface of CZTS thin films. This may be because the plasma plume had nucleation process during the pulsed laser deposition. At the laser incident energy of $3 \text{ J}\cdot\text{cm}^{-2}$, the CZTS thin film had relatively high uniformity and a quite flat surface.

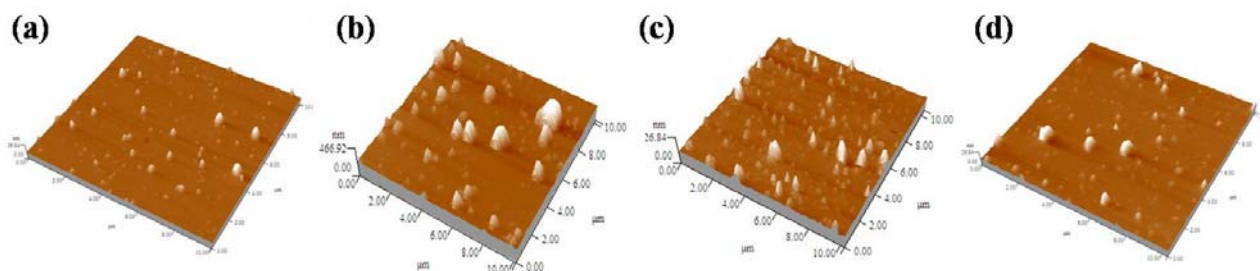


Fig.3. AFM 3-dimension surface images for an area of $10 \times 10 \mu\text{m}^2$ of CZTS thin films at the different incident laser energy

(a) $3 \text{ J}\cdot\text{cm}^{-2}$; (b) $4 \text{ J}\cdot\text{cm}^{-2}$; (c) $5 \text{ J}\cdot\text{cm}^{-2}$; (d) $6 \text{ J}\cdot\text{cm}^{-2}$.

Band gap of CZTS thin films. The band gaps of CZTS thin films were estimated by extrapolating the linear region of a plot of the absorbance squared $(\alpha h\nu)^2$ versus energy $h\nu$ as shown in Fig.4. The band gaps of CZTS thin films were 1.72, 1.37, 1.25 and 1.11 eV, corresponding to the incident laser energy of 3, 4, 5 and $6 \text{ J}\cdot\text{cm}^{-2}$, respectively. The band gap decreased with the increase of the laser incident energy. The result was consistent with that of XRD.

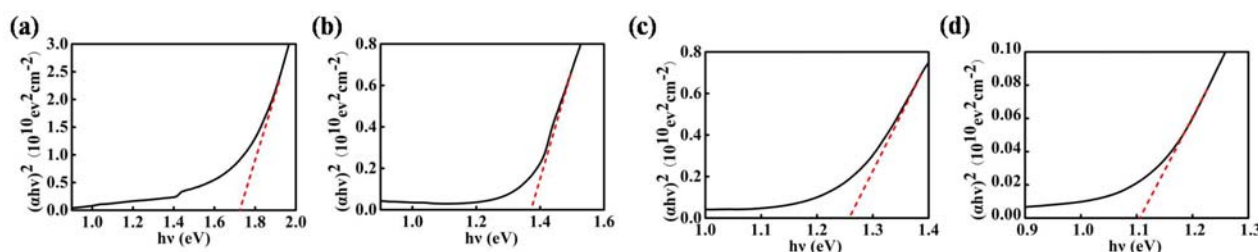


Fig.4. Plot of $(\alpha h\nu)^2$ versus $h\nu$ for CZTS thin films at different laser incident energies

(a) $3 \text{ J}\cdot\text{cm}^{-2}$; (b) $4 \text{ J}\cdot\text{cm}^{-2}$; (c) $5 \text{ J}\cdot\text{cm}^{-2}$; (d) $6 \text{ J}\cdot\text{cm}^{-2}$.

Summary

The CZTS thin films were successfully grown on the glass substrates by pulsed laser deposition method with varying the laser incident energy from from $3 \text{ J}\cdot\text{cm}^{-2}$ to $6 \text{ J}\cdot\text{cm}^{-2}$ at the interval of $1 \text{ J}\cdot\text{cm}^{-2}$. At the laser incident energy of $5 \text{ J}\cdot\text{cm}^{-2}$, the chemical composition of the CZTS thin film was $\text{Cu}_{2.15}\text{Zn}_{1.00}\text{Sn}_{1.17}\text{S}_{3.84}$ in a nearly stoichiometric relation except slightly Cu-rich and S-poor. The CZTS thin films at different laser incident energy had strong preferentially oriented along (112) plane in XRD results. The band gaps of CZTS thin films were 1.72, 1.37, 1.25 and 1.11 eV, corresponding to the incident laser energy of 3, 4, 5 and $6 \text{ J}\cdot\text{cm}^{-2}$, respectively.

Acknowledgment

This work is financially supported by the National Natural Science Foundation of China (51072043).

References

- [1] M.A. Contreras, K. Ramanathan, J.AbuShama, F. Hasoon, D.L. Young, B. Egass, R. Noufi: Prog. Photovolt Vol. 13 (2005), p. 119.
- [2] Qijie Guo, H. W. Hillhouse, R. Agrawal: J. Am. Chem. Soc Vol. 131 (2009), p. 11672.
- [3] K. Ito, T. Nakazawa: Jpn. J. Appl. Phys Vol. 27 (1988), p. 2094.
- [4] H. Katagiri, K. Saitoh, T. Washio, H. Shinohara, T. Kurumadani, S. Miyajima: Sol. Energy Mater. Sol. Cells Vol. 65 (2001), p. 141.
- [5] T. Tanaka, A. Yoshida, D. Saiki, K. Saito, Qixin Guo, M. Nishio, T. Yamaguchi: Thin Solid Films Vol. 518 (2010), p. S29.
- [6] N. Kamoun, H. Bouzouita, B. Rezig: Thin Solid Films Vol. 515 (2007), p. 5949.

- [7] J.S. Seol, S.Y. Lee, J.C. Lee, H.D. Nam, K.H. Kim: Sol. Energy Mater. Sol. Cells Vol. 75(2003), p. 155.
- [8] T. Tanaka, T. Nagatomo, D. Kawasaki, M. Nishio, Q. Guo, A. Wakahara, A. Yoshida, H. Ogawa: J. Phys Chem. Solids Vol. 66 (2005), p. 1978.
- [9] C.P. Chan, H. Lam, C. Surya: Sol. Energy Mater. Sol. Cells Vol. 94 (2010), p. 207.
- [10] K. Oishi, G. Saito, K. Ebina, M. Nagahashi, K. Jimbo, W.S. Maw, H. Katagiri, M. Yamazaki, H. Araki, A. Takeuchi: Thin Solid Films Vol. 517 (2008), p. 1449.
- [11] A.V. Moholkar, S.S. Shinde, A.R. Babar, K.U. Sim, Y.B. Kwon, K.Y. Rajpure, P.S. Patil, C.H. Bhosale, J.H. Kim: Sol. Energy Vol. 85 (2011), p. 1354.
- [12] S.M. Pawar, A.V. Moholkar, I.K. Kim, S.W. Shin, J.H. Moon, J.I. Rhee, J.H. Kim: Curr. Appl. Phys. Vol. 10 (2010), p. 565.
- [13] Lin Sun, Jun He, Hui Kong, Fangyu Yue, Pingxiong Yang, Junhao Chu: Sol. Energy Mater. Sol. Cells Vol. 95(2011), p. 2907.
- [14] Chengwu Shi, Gaoyang Shi, Zhu Chen, Renjie Sun, Mei Xia: J. Chin. Ceram. Soc. Vol. 39 (2011), p. 1108.